IoT Platform Enabling Artificial Intelligence for Predicting Blocking in OWC

Francisco Javier Simón Fernández, Alejandro Lopez Barrios*, Máximo Morales-Céspedes*
*Department of Signal Theory and Communications. Universidad Carlos III de Madrid, Leganés, Spain
Email: 100472842@alumnos.uc3m.es, albarrios@tsc.uc3m.es, mmcesped@ing.uc3m.es

***Abstract*—Optical wireless communications (OWC) have been proposed for providing connectivity in environments where implementing traditional radiofrequency (RF) systems is challenging or even banned, as occurs in several industrial scenarios such as mining, tunnel construction or oil&gas factories among others. Specifically, OWC results suitable for providing IoT, positioning and resource monitoring services. However, they are extremely sensitive to blocking effects, which may easily appear in the optical domain because of the presence of people or machinery. In this work, we propose an IoT platform to obtain information about the environment such as illumination level, distance to transmitter or angles of radiance and incidence to feed artificial intelligence (AI) algorithms for predicting blocking. Once a realistic dataset is obtained, the blocking prediction is analyzed for machine learning and adaptive filters. The obtained results show that blocking effects can be predicted within a window of 100 ms subject to an accuracy greater than 80% by exploiting the measured IoT parameters.**

I. Introduction

Optical wireless communications (OWC) have been proposed as an alternative technology for providing connectivity in industrial scenarios. Specially, in those where traditional radiofrequency (RF) systems are limited or banned as occurs in oil&gas plants, tunnel construction or some hospital areas [1]. In this sense, OWC have been proposed for internet of things (IoT) applications, positioning or monitoring of production resources among others. Notice that beyond the original purposes of these applications, they can be also employed for generating realistic datasets that feed artificial intelligence (AI) algorithms to improve the performance of OWC networks [2].

Focussing on industrial environments, blocking and shadowing play a major role since they directly impact in the reliability of the connectivity [3], [4]. For instance, blocking may cancel the monitoring of the position of autonomous vehicles, which may lead to a loss of vehicle control. However, most of the available works treat blocking as an instantaneous and unpredictable effect. On the other hand, realistic measurements show that blocking and shadowing do not occur instantaneously, which make them potentially predictable [3]. Therefore, the measurement and instrumentation of additional parameters such as illumination, height or incidence angle represents and an opportunity for predicting blockages.

At this point, OWC systems can be employed to obtain information about the propagation environment through an IoT platform that converges to a database. This set of information can be exploited for feeding AI algorithms. Although learning algorithms have been proposed for channel estimation, optimizing modulation schemes or reducing the impact of non-linearities in OWC, e.g., [5], [6], [7], they are mainly based on synthetic datasets. In this sense, realistic measurements are required to take into consideration parameters such as illumination, reflections or the presence of people/machinery [8]. Then predicting the blockage of the optical channel enables to implement signal processing methodologies to minimize their effects. For instance, applying horizontal handover to a neighbouring optical transmitter following a topological approach [9], selecting other photodiode exploiting an angular diversity structure [10] or applying a vertical handover to a RF umbrella network [11].

In this work, we propose an IoT platform for measuring parameters such as illumination, angles of radiance and incidence, lens, etc., that feed AI algorithms to predict optical blockage. The contributions of this work can be summarized as follows,

1) A data-driven approach based on exploiting the instrumentation of a consumer device is proposed to effectively predicting the presence of blockage. In contrast to previous works, it is demonstrated that blockage cannot be managed as an instantaneous effect while predicting it within a guard time to activate handover or diversity mechanisms before the optical signal is blocked.
2) Learning algorithms such as decision trees and random forest learning methods, and least mean squares (LMS) and recursive least squares (RLS) adaptive filters are analyzed. To avoid the instantaneous classification of the channel, either blocked or not, the sliding window technique is employed to estimate the blocking probability at future time $t+n$, where t and n denotes the instantaneous time and window size, respectively.

The proposed methodology is evaluated in a testbed that emulates an industrial OWC network in which high-power LEDs provide 100 kbps data rate. The obtained results have been evaluated for a sliding window of 100 ms, demonstrating a blocking prediction accuracy about 80% subject to low levels of false alarm.

This work is supported by the projects funded by MICIU/AEI/10.13039/501100011033 "SOFIA" (PID2023-147305OB-C31), project "PASSIONATE" funded by the CHISTERA grant CHIST-ERA-22-WAI-04, by AEI PCI2023-145990-2 and in part by TUCAN6-CM (TEC-2024/COM460), funded by CM (ORDEN 5696/2024). The work of M. Morales-Céspedes is supported by Ramón y Cajal RYC2022-036053-I funded by MICIU/AEI/10.13039/501100011033 and FSE+.

II. System model

We consider an OWC system composed of a single optical transmitter providing a coverage footprint with a radius of 2 m as depicted in Fig. 1. The transmitted signal follows a on-off keying (OOK) modulation denoted by x. The signal corresponds to N_p pilot symbols employed for estimating the optical channel. Then, the signal received by the photodiode can be written as

$$y = hx + n, \tag{1}$$

where h is the optical channel and n is additive white Gaussian noise (AWGN) with zero mean and variance σ_n^2, which comprises the effects of both thermal and shot noise.

From a theoretical perspective, the line-of-sight (LoS) contribution of the optical channel as a DC gain is given by

$$h = \begin{cases} \frac{\gamma A(m+1)}{2\pi d_{lk}^2}\cos^m(\phi)\,T(\varphi)\cos(\varphi) & \text{if } 0 \le \Psi \le \varphi \\ 0 & \text{if } \Psi > \varphi, \end{cases} \tag{2}$$

where γ and A are the responsivity and area of detection of the photodiode, respectively, d is the distance between optical transmitter ad user, ϕ is the radiance angle, φ is the incident angle, Ψ corresponds to the field of view (FoV) and m is the order of Lambertian emission, where $\phi_{1/2}$ is the radiation semi-angle so that $m = -\frac{\ln 2}{\ln\cos(\phi_{1/2})}$. Moreover, in (2), $T(\varphi)$ denotes the optical response of the filter and concentrator.

III. Measurement Set-up

A. Transmitter

The transmitter corresponds to a chip on board (CoB) LED CLU038-1208 of Citizen Electronics [12] that is polarized with a mean forward current and voltage equal to 720 mA and 36 V, respectively, which provides a 2940 lm luminous flux. On the other hand, the transmitted signal corresponds to a 5 V_{pp} OOK modulation. Specifically, a signal composed of 128 bits is transmitted for estimating the channel state information at the receiver side. A driver circuit as depicted in Fig. 2 is employed to modulate the 5 V_{pp} OOK signal from a microcontroller at baud rate of 115.2 kbauds to the LED employing the universal receiver-transmitter (UART) module. Notice that the forward current modifies the illumination level while the amplitude of the transmitted signal determines the channel estimation as described in Fig. 2.

B. Channel

The measurements are obtained in the laboratory of the communications group of Universidad Carlos III de Madrid. The LED is located in a height equal to 3 m. Although the LoS represents the main contribution to the optical channel, other effects such as shadowing, reflections on wall and furniture or turbulence may appear [13]. Notice that these effects are not considered by the Lambertian model in (2), while they may provide useful information for predicting blockage to AI algorithms. Moreover, the illumination and noise can be also affected by the weather (sunny or cloudy). For generating the blocking effects both a 1 m $\times$ 1 m $\times$ 1 m cardboard box and human activity crossing the optical footprint are considered during the measurement campaign. It is assumed that each blockage comprises a period greater than 250 msec.

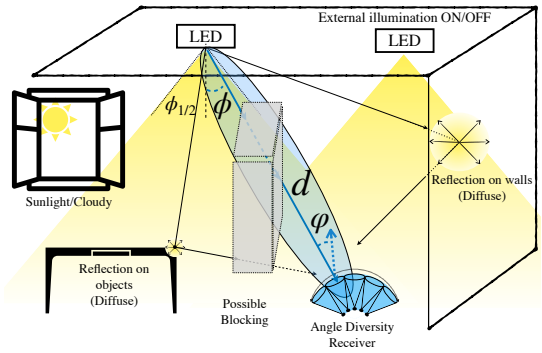

Fig. 1. OWC realistic scenario subject to blocking effects.

C. Receiver

The receiver is composed of several sensors to obtain information about the propagation environment. Specifically, the following parameters are measured in the proposed IoT platform.

- **Received signal.** For signal detection the amplified photodetector PDA100A2 [14] of Thorlabs is employed. This photodetector is composed of a photodiode connected to a switchable gain transimpedance amplifier (TIA). Specifically, for a TIA gain equal to 30 dB, it provides a bandwidth of 260 kHz, which obtains a trade-off between gain and bandwidth for the transmitted signal. This photodetector is typically employed in OWC applications. For a gain of 30 dB, the measurements are subject to an offset of $\pm$8 mW and a noise equivalent power equal to $3.36 \cdot 10^{-12}$ $\frac{\text{W}}{\sqrt{\text{Hz}}}$. The output of the photodetector is digitalized at the receiver side to apply signal processing and channel estimation.
- **Illumination.** The illumination level is measured employing the sensor BH1750. It provides a resolution of 1-65535 lux using the I2C bus interface. It is worth remarking that BH1750 corresponds to a low-cost sensor typically implemented in consumer devices subject to an error equal to $\pm$10%.
- **Height of the receiver.** The TeraRanger EVO 60 m is employed to measure the distance between receiver and ceiling. This value is related with the illumination level and the angles of radiance and incidence. This sensor measures the distance employing the time of flight using LED technology instead of a laser subject to $\pm$4 cm accuracy in the first 14 m.
- **Angles of radiance/incidence.** The values of these angles are treated as inputs of the AI algorithms to analyze their impact in blocking effects. A digital inclinometer subject to a $\pm 0.2^\circ$ error is employed for measuring the irradiance and incidence angle.
- **Lens**. The use of lenses is considered to analyze the impact of the FoV in blocking effects. Specifically, the case of no using lens and uncoated plano-convex lenses with focal distance 25.4 mm and 100 mm are analyzed.

The average value of the optical channel corresponds to a voltage of 1.2 V at the output of the TIA, with illumination levels of 160 lux and 50 lux when external lighting is on and

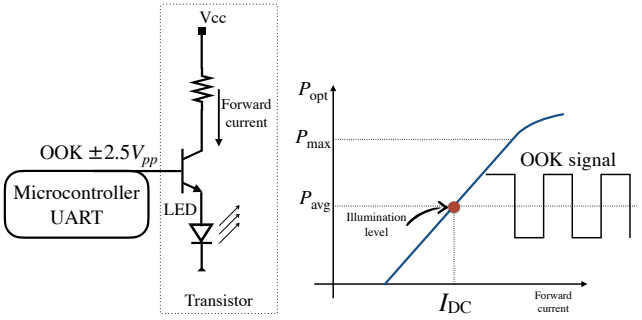

Fig. 2. Architecture of the OWC-IoT transmitter.

off, respectively. Channel blockage induces fading greater than 12 dB, resulting in illumination levels of 80 lux and 35 lux. In this regard, the instrumentation employed at the receiver for measuring blockages is subject to an error that is considered negligible.

IV. Methods for predicting blockage in OWC

The prediction of blockage is based on two approaches machine learning and adaptive filters. The set of input parameters are denoted by $\mathbf{x}(t)$, which comprises all the parameters measured by the IoT platform, and the output parameter is denoted by $y(t)$. Moreover, the error $e(t)$ is given by $\hat{y}$ and y correspond to the estimated and true value, respectively.

A. Machine learning methods

1) Decision trees: The decision tree recursively partitions the feature space $\mathbf{x}$ into homogeneous regions with respect to the output variable y [15]. At each internal node, the feature x_j and the threshold t_j are selected to maximize information gain or, equivalently, minimize node impurity. A common criterion is the Gini index,

$$G = 1 - \sum_{k=1}^{K} p_k^2, \tag{3}$$

where p_k corresponds to the percentage of samples belonging to class k within the node. Notice that for the binary case, i.e., $K = 2$, the tree depends on either blocking or not. For instance, if the set of input parameters satisfies some criterion, then blocking occurs or it is predicted.

In such a way, the model generates an interpretable decision hierarchy, allowing for the identification of which variables and physical thresholds are most important and relevant to the presence of blocking. However, decision trees tend to overfit if their depth or the minimum number of samples per node is not limited, which is controlled through regularization.

2) Random Forest: The random forest goes beyond the principle of the decision tree through an ensemble approach (bagging) [16], in which M independent trees are trained on random subsets of the dataset and the features. Each tree $f_m(x)$ produces an individual prediction, and the final model performs an average or majority vote,

$$\hat{y} = \frac{1}{M} \sum_{m=1}^{M} f_m(x). \tag{4}$$

This process introduces diversity among the base models, reducing variance and improving stability against noise or correlations between variables. Focussing on OWC, this property results useful, due to the rapid fluctuations and mutual dependencies of the optical power and angle measurements [10]. It obtains a trade-off between precision and robustness, serving as a common benchmark in binary classification tasks

B. Adaptive filters

In real-world environments such as factories, tunnels, or logistics platforms, the optical channel conditions vary over time due to changes in geometry, ambient lighting, or interference. To maintain the performance without the need for frequent retraining of the offline classifier, adaptive models are capable of adjusting their parameters in real time. In this work, two classic adaptive filtering algorithms are employed; least mean squares (LMS) and recursive least squares (RLS) [17]. Both operate by estimating an output $\hat{y}(t)$ from the linear combination of an input feature vector $\mathbf{x}(t)$ and an adaptive weight vector $\mathbf{w}(t)$. That is,

$$\hat{y}(t) = \mathbf{w}^T(t) \cdot \mathbf{x}(t). \tag{5}$$

The objective of both algorithms is to minimize the instantaneous error $e(t)$ between the prediction and the desired signal, updating the weight vector $\mathbf{w}(t)$ at each iteration.

1) Least mean squares: The LMS algorithm implements a stochastic gradient descent rule. It is notable for its low computational complexity, $O(N)$, making it ideal for implementations on lightweight hardware. The update rule is given by

$$\mathbf{w}(t+1) = \mathbf{w}(t) + \mu e(t)\mathbf{x}(t). \tag{6}$$

The behavior of the LMS algorithm is determined by the learning step size μ. A high value of μ accelerates adaptation to rapid changes but may introduce instability or estimation noise (misadjustment), whereas a reduced value of μ ensures smooth and stable convergence at the cost of a slower response to abrupt channel variations.

2) Recursive Least Squares: Unlike the LMS algorithm, the RLS algorithm takes into account the correlation structure of the input data to minimize a weighted least squares error [16]. This allows for a much higher convergence speed, especially when the inputs are correlated, although it involves a higher computational cost $O(N^2)$. For RLS, the weight update can be written as

$$\mathbf{w}(t) = \mathbf{w}(t-1) + \mathbf{k}(t)e(t), \tag{7}$$

where $e(t)$ is the a priori estimation error, i.e., $e(t) = d(t) - \mathbf{w}(t-1)\mathbf{x}(t)$., and k is the gain vector update, which is defined as,

$$\mathbf{k}(t) = \frac{\mathbf{P}(t-1)\mathbf{x}(t)}{\lambda + \mathbf{x}(t)\mathbf{P}(t-1)\mathbf{x}(t)}, \tag{8}$$

where λ is the forgetting factor.

The critical design parameter in the RLS algorithm is the forgetting factor λ, typically within the range $(0,1]$; whereas a value of $\lambda \approx 1$ provides the algorithm with a long memory, rendering it robust against noise but slow to decay past states, reducing λ assigns less weight to older samples, thereby

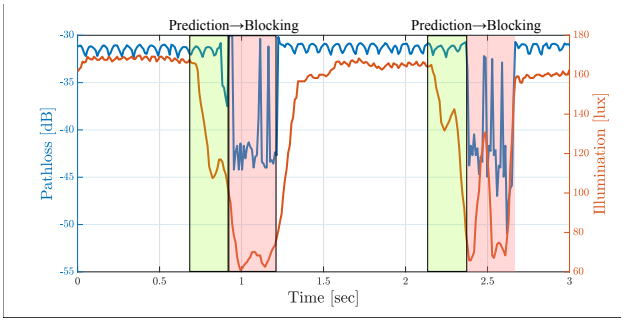

(a) External illumination on

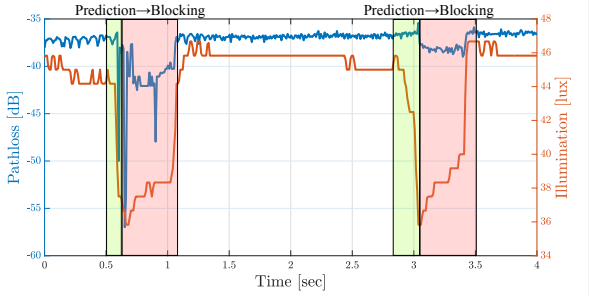

(b) External illumination off

Fig. 3. Evolution of channel and illumination for blocking prediction subject to different illumination levels.

enabling rapid tracking of abrupt change such as sudden signal blocking at the expense of increased sensitivity to noise.

C. Sliding window

The described models classify the state of the channel at the instantaneous time. Although this approach is useful for managing the instantaneous channel, it implies that detection occurs simultaneously with the loss of connection following a blockage. To address this, the use of a sliding window technique is proposed, where the learning objective is to estimate the probability of blockage at a future time $t+n$. This strategy provides the system with a guard time to activate handover or diversity mechanisms before service interruption occurs. The difficulty of this strategy lies in the fact that the model must infer future events based solely on subtle trends, e.g., the derivative of received power or angular variations. presented in the current data.

In this work, we consider a 100 ms sliding window. Measurement results have show that this value provides a trade-off between detection and false alarm. Moreover, notice that a 100 ms window involves the transmission of about 1450 bytes approximately for a data rate of 115.2 Kbits/sec, which corresponds to a prediction window enough to avoid the loss of packets because of blocking effects.

D. Methodology

The workflow for training and validation of the predictive models combines stages of data processing, offline supervised adjustment, and online adaptive evaluation. By reproducing the entire blocking prediction cycle, this study benchmarks the efficacy of static models against dynamic filters under realistic conditions. The phases of the process are described in the following.

1) **Data Acquisition and Labeling**. First, the physical variables of the optical channel $\mathbf{x}(t)$ (received power, angles, noise, etc.) are recorded along with the binary label $y(t)$ indicating the link status (blocked / non-blocked). This label is obtained by applying an objective criterion based on performance indicators or a power threshold $P_r(t)$, ensuring temporal correspondence between the measurements and the true link status.
2) **Preprocessing.** Raw data undergo cleaning and normalization. Temporal synchronization, outlier removal, and magnitude standardization are performed. Furthermore, feature engineering techniques are applied to capture temporal patterns, such as the calculation of derivatives and rolling statistics over time windows.
3) **Data Partitioning**. A sequential partitioning scheme (time-series split) is used to divide the data into training, validation, and testing sets. Unlike random splitting, this preserves the temporal order, ensuring that the system is evaluated by predicting future events based on past data, thereby simulating a real-world scenario.
4) **Offline Training.** The training set is utilized within a k-fold cross-validation ($k=5$ is assumed). This method maximizes the use of available data for robust hyperparameter selection, while reserving the rigorous temporal evaluation for the final independent test set. Hyperparameters are optimized via grid search, selecting the configuration that minimizes the mean error before final evaluation on the test set.
5) **Online Deployment and Comparison**. Once the optimal static model is trained, it is deployed in inference mode on new observations. Simultaneously, the LMS and RLS adaptive filters are executed. Unlike a hybrid fusion, here both systems operate concurrently to determine which approach offers a better performance, i.e., the generalization capability of the supervised model or the tracking speed of the adaptive filter.
6) **Model Evaluation**. Finally, performance metrics are monitored against blocking events not seen during training. This phase allows for a comparison between the static model and the adaptive filters, validating which of the two strategies is most suitable for predicting optical blockage in each operational scenario.

V. Obtained Results

The evolution of the optical channel, i.e., the path loss (see (2)) and illumination during the measurement process is depicted in Fig. 3 for different environmental conditions, e.g., external illumination on/off. It can be seen that blocking effects are not instantaneous; both path loss and illumination exhibit distinct behaviors. Specifically, the illumination is affected by blockage sooner than the optical channel. As a consequence, blocking of the optical channel can be predicted by the illumination level. Notice that blocking generates shadows that can be detected by the illumination sensor before the optical channel is completely affected by blocking. It can

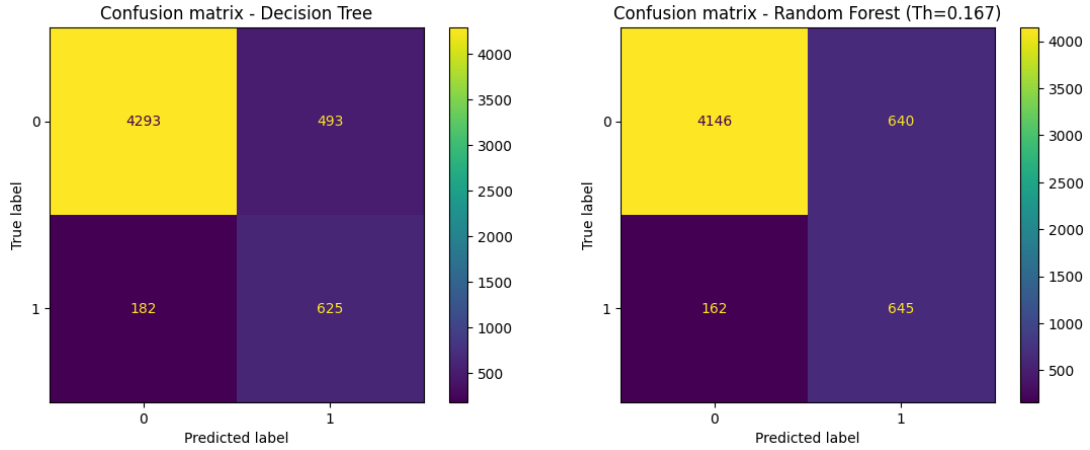

(a) Machine learning. Decision trees.

(b) Machine learning. Random forest.

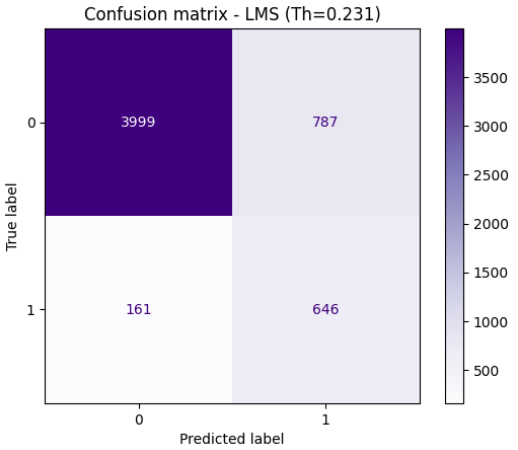

(c) Adaptive filters. LMS.

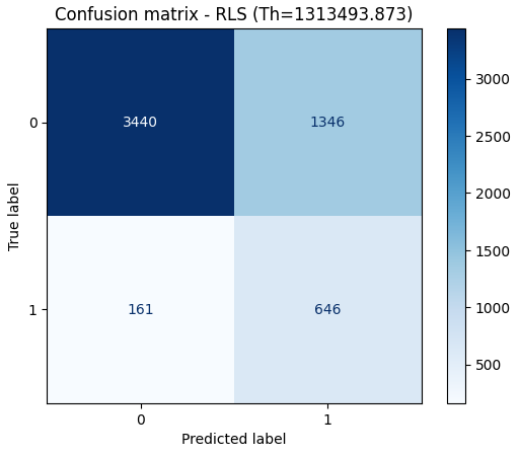

(d) Adaptive filters. RLS.

Fig. 4. Confusion matrices for the proposed learning methods and adaptive filters.

be also seen that it becomes more predictable when external illumination is present, as it can be quantified by simply measuring light levels. Moreover, the shadows detected by the illumination sensor depends of parameters such as height, angles of irradiance/incidence or the use of optical lenses.

In the following, we analyze the performance of the considered adaptive and learning schemes for predicting blockage. The simulation results consider the transmission of 5593 frames measured by the proposed IoT-OWC platform. First, the confusion matrices for each of the considered prediction blocking schemes with a slide window of 100 ms are depicted in Fig. 4. Moreover, the accuracy, precision, recall, F1 score and area under the receiver operating characteristic curve (AUC-ROC) parameters of each prediction blocking scheme are summarized in Fig. I.

Focussing on the proposed learning methods, in Fig. 4(a) and Fig. 4(b), it can be seen that random forest detects more true blockages than decision trees, from 625 to 645, at the cost of increasing the number of false positives. As a consequence, decision trees method achieves a slightly greater accuracy and precision, while reducing the recall. While decision tree and random forest models achieve near-perfect performance in static classification (AUC-ROC ≈ 1.0), i.e., without considering a slide window for predicting blockage, the introduction of a 100 ms sliding window for prediction reduces this value to 0.837. This occurs because both learning methods generates rigid partitions of the space based on instantaneous values. Then, when attempting to predict the future $(t+n)$, the correlation between the current signal value and the future state decreases, causing many samples to fall on the wrong side of the decision boundary.

In Fig. 4(c), it can be seen that the LMS scheme provides to be a highly efficient solution. With an AUC of 0.86, it effectively captures the channel trend, adapting to changes without the need for complex training. Calibration allows it to meet safety requirements while assuming a moderate false

TABLE I
PERFORMANCE COMPARISON OF LEARNING METHODS AND ADAPTIVE FILTERS FOR BLOCKING PREDICTION IN OWC.

	Decision Trees	**Random Forest**	**LMS**	**RLS**
Accuracy	0.8793	0.8566	0.8305	0.7306
Precision	0.5590	0.5019	0.4508	0.3243
Recall	0.7745	0.7993	0.8005	0.8005
F1	0.6494	0.6166	0.5768	0.4616
AUC-ROC	0.8370	0.8777	0.8644	0.8234

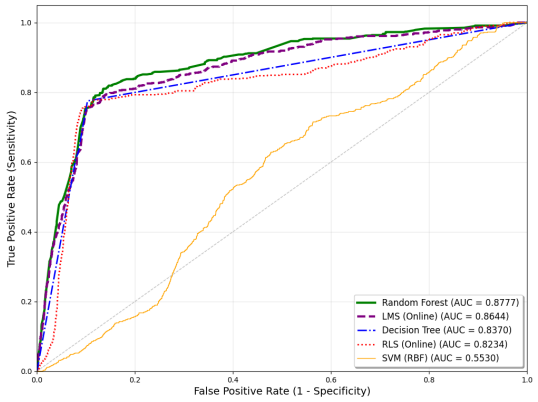

Fig. 5. Relation of the true/false positive rate for the considered adaptive filters and learning methods.

alarm rate, i.e, detecting 80% of blockages with a precision about 45%. The greatest advantage of this model is its linear computational cost. It is a lightweight and fast algorithm, making it suitable for embedded systems where heavy models cannot be used. Despite its greater theoretical complexity, RLS achieves lower performance compared to the LMS in this scenario (see Table I). Its rapid convergence speed makes it more sensitive to channel noise, generating a higher number of false alarms without providing an improvement in overall discrimination capability, i.e., lower precision and AUC-ROC.

The relation between sensitivity and specificity is analyzed for the proposed adaptive filters and learning methods as well as for the use of a vector support machine (SVM) in Fig. 5. It can be seen that SVM achieves a poor performance due to high sensitivity to noisy and overlapping date. That is, SVM does not work properly for analyzing the signal associated to blocking in OWC, which basically follows a predefined pattern subject to overlapping data. On the other hand, LMS adaptive filter results suitable for predicting blockage in comparison with RLS and also with other learning algorithms. It can be also seen that random forest outperforms decision trees since it reduces overfitting and variance by averaging multiple decision trees. As a consequence, it results suitable for predicting a repetitive pattern such as blocking effects in OWC.

VI. Conclusions

In this paper, an IoT platform for OWC is presented to generate realistic datasets to enable the prediction of blocking based on AI algorithms. First, the set of parameters that compose this dataset are described, specifying the employed sensors for measuring purposes. After that, decision trees and random forest machine learning algorithms as well as LMS and RLS adaptive filters are formulated to predict blocking applying the concept of sliding window. These methods are evaluated employing a dataset composed of 5593 samples dataset. It is shown that learning methods and LMS adaptive filter achieve a blocking prediction accuracy above 80% subject to a low probability of false alarm.

Further works will consider the blockage in practical environments beyond the datasets obtained in the laboratory. Specifically, the prediction of blockage will be analyzed during tunnel construction considering distinct prediction sliding windows as well as long short-term memory (LSTM) or gated recurrent uni (GRU) algorithms. Moreover, classification and tracking of blocking targets will be considered exploiting the datasets obtained in hardware testbeds.

References

[1] H. Yang, W.-D. Zhong, C. Chen, and A. Alphones, "Integration of visible light communication and positioning within 5G networks for internet of things," *IEEE Network*, vol. 34, no. 5, pp. 134–140, 2020.

[2] A. Celik, I. Romdhane, G. Kaddoum, and A. M. Eltawil, "A top-down survey on optical wireless communications for the internet of things," *IEEE Communications Surveys & Tutorials*, vol. 25, no. 1, pp. 1–45, 2023.

[3] T. Pal, A. Singh, V. A. Bohara, and A. Srivastava, "Impact of time-varying dynamic human blockages on indoor visible light communication system," *IEEE Transactions on Wireless Communications*, vol. 23, no. 9, pp. 10 562–10 574, 2024.

[4] A. Singh, H. B. Salameh, M. Ayyash, and H. Elagla, "Characterization of dynamic blockages for VLC-enabled indoor industrial networks," *IEEE Systems Journal*, vol. 18, no. 4, pp. 2173–2176, 2024.

[5] N. A. Amran, M. D. Soltani, M. Yaghoobi, and M. Safari, "Learning indoor environment for effective LiFi communications: Signal detection and resource allocation," *IEEE Access*, vol. 10, pp. 17 400–17 416, 2022.

[6] A. Ullah, W. Choi, and S. Coleri, "Path loss estimation and jamming detection in hybrid RF-VLC vehicular networks: A machine-learning framework," *IEEE Sensors Journal*, vol. 23, no. 24, pp. 31 325–31 336, 2023.

[7] D. Gao, Q. Guo, M. Jin, Y. Yu, and J. Xi, "Adaptive extreme learning machine-based nonlinearity mitigation for LED communications," *IEEE Journal of Selected Topics in Quantum Electronics*, vol. 27, no. 2, pp. 1–9, 2021.

[8] M. Morales-Céspedes, J. Pérez-Aracil, A. García-Armada, and S. Salcedo-Sanz, "Learning for visible light communications: Potential scenarios and applications," *IEEE Consumer Electronics Magazine*, vol. 14, no. 6, pp. 10–25, 2025.

[9] R. Torrea-Duran, M. Morales Céspedes, J. Plata-Chaves, L. Vandendorpe, and M. Moonen, "Topology-aware space-time network coding in cellular networks," *IEEE Access*, vol. 6, pp. 7565–7578, 2018.

[10] C. Chen, W.-D. Zhong, H. Yang, S. Zhang, and P. Du, "Reduction of sinr fluctuation in indoor multi-cell VLC systems using optimized angle diversity receiver," *Journal of Lightwave Technology*, vol. 36, no. 17, pp. 3603–3610, 2018.

[11] A. A. Qidan, M. Morales-Cespedes, and A. G. Armada, "The role of WiFi in LiFi hybrid networks based on blind interference alignment," in *2018 IEEE 87th Vehicular Technology Conference (VTC Spring)*, 2018, pp. 1–5.

[12] "CitiLed COB Series CLU04848-1212C4," Citizen, Datasheet, 2019. [Online]. Available: https://bit.ly/2EryDsV

[13] P. P. Játiva, C. A. Azurdia-Meza, I. Sánchez, F. Seguel, D. Zabala-Blanco, A. D. Firoozabadi, C. A. Gutiérrez, and I. Soto, "A VLC channel model for underground mining environments with scattering and shadowing," *IEEE Access*, vol. 8, pp. 185 445–185 464, 2020.

[14] "PDA100A2 - Si Fixed Gain Detector," Thorlabs, Datasheet, 2019. [Online]. Available: https://www.thorlabs.com/thorproduct.cfm?partnumber=PDA100A2

[15] L. Breiman, J. Friedman, R. Olshen, and C. Stone, *Classification and regression trees*. Belmont: Wadsworth, 1984.

[16] I. Goodfellow, Y. Bengio, and A. Courville, *Deep Learning*. MIT Press, 2016.

[17] I. Haykin, *Adaptive Filter Theory, 5th ed.* Pearson Education, 2014.